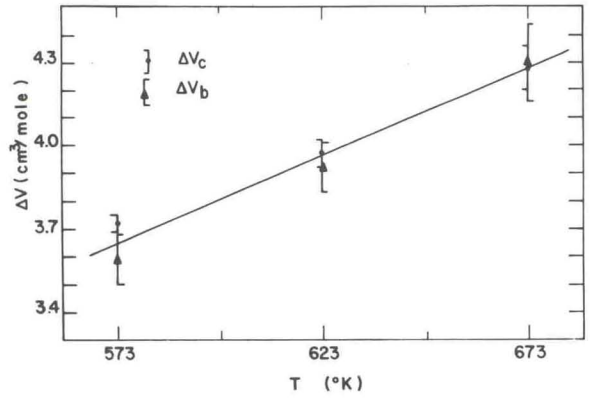

FIG. 3. Variation of activation volume with temperature.

brought to the same common pressure. The activation enthalpies ΔH_c and ΔH_b and the frequency factors D_{0c} and D_{0b} obtained by doing a linear least-squares fit to these plots are given in Table III, together with the zero-pressure values from previous work.[10]

The variation of ΔH_c and $\ln D_{0c}$ with pressure is shown in Fig. 6, and that of ΔH_b and $\ln D_{0b}$ with pressure is shown in Fig. 7. Within the experimental limits of error, ΔH_c and ΔH_b are independent of pressure. This can also be seen by considering the variation of activation volume ΔV with temperature T. According to Eq. (7), the intercept

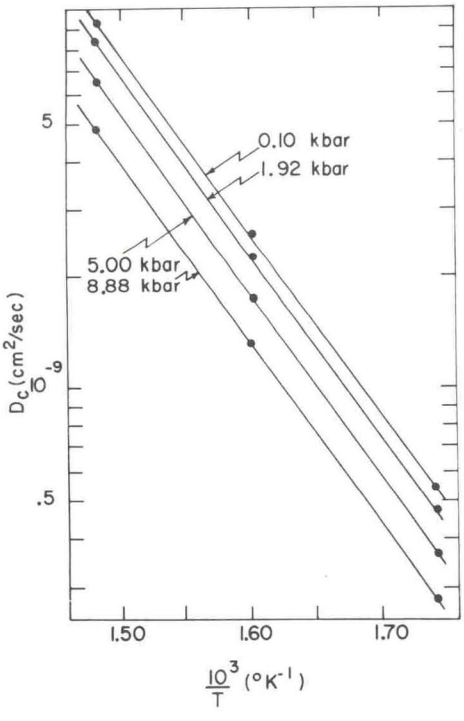

FIG. 4. Arrhenius plots of $\ln D_c$ vs $1/T$, for self-diffusion in zinc at pressures of 0.10, 1.92, 5.00, and 8.88 kbar.

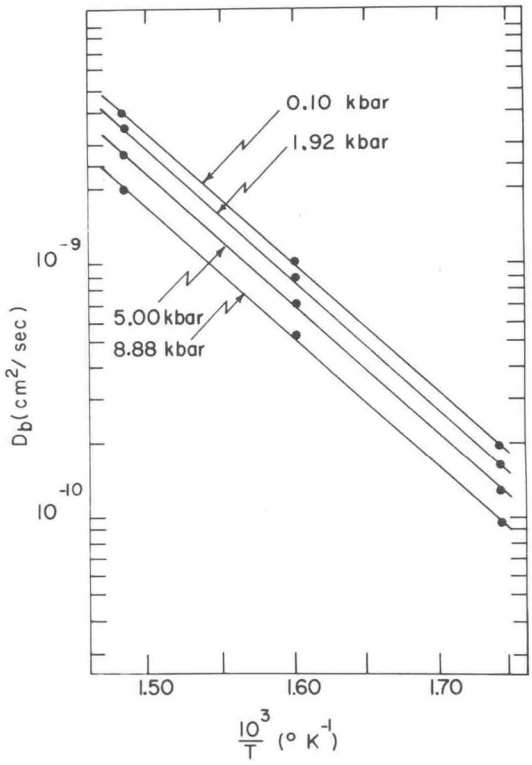

FIG. 5. Arrhenius plots of $\ln D_b$ vs $1/T$ for self-diffusion in zinc at pressures of 0.10, 1.92, 5.00, and 8.88 kbar.

of the plot of ΔV vs T in Fig. 5 is simply $(\partial \Delta H/\partial p)_T$. The least-squares fit to the activation-volume data gives $(\partial \Delta H/\partial p)_T = -0.003 \pm 0.3$ cm^3/mole, i.e., $(\partial \Delta H/\partial p)_T \simeq 0$.

On the other hand, the frequency factors D_{0c} and D_{0b} decrease with pressure. The frequency factor D_0 is defined as $D_0 = f a_0^2 \nu e^{\Delta S/R}$, where f is the correlation factor, a_0 is the effective jump distance, ν is the barrier attack frequency (comparable to the Debye frequency), and ΔS is the activation entropy. Differentiating $\ln D_0$ with respect to pressure and realizing[13] that the self-diffusion coefficients are determined by serial sectioning at room temperature and pressure, we then have

TABLE III. Activation enthalpies and frequency factors at various pressures.

p (kbar)	ΔH_c (kcal/mole)	ΔH_b (kcal/mole)	$\ln D_{0c}$	$\ln D_{0b}$
0.10	21.96 ± 0.08	23.47 ± 0.15	−2.06 ± 0.04	−1.77 ± 0.12
1.92	22.10 ± 0.10	23.70 ± 0.11	−2.08 ± 0.07	−1.72 ± 0.09
5.00	22.10 ± 0.08	23.50 ± 0.15	−2.31 ± 0.04	−2.09 ± 0.12
8.88	22.00 ± 0.10	23.44 ± 0.25	−2.68 ± 0.08	−2.47 ± 0.20
0.00[a]	21.90 ± 0.15	23.48 ± 0.15	−2.04 ± 0.08	−1.68 ± 0.18

[a]Obtained from Ref. 10.

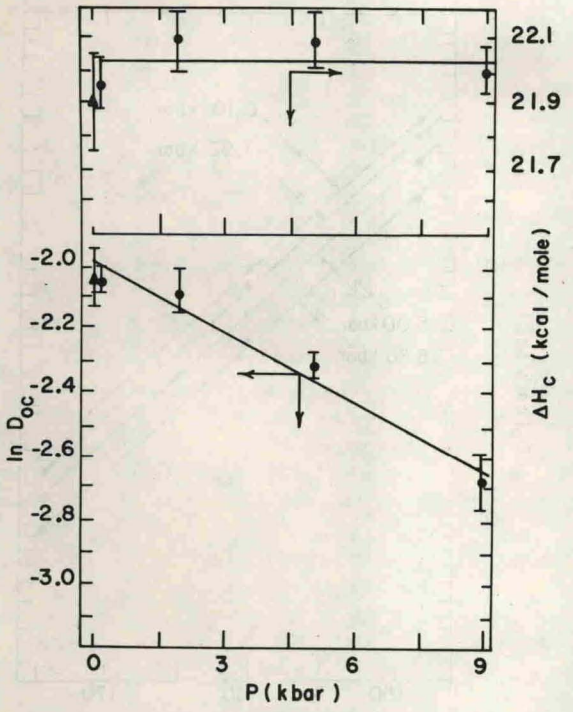

FIG. 6. Variation of ΔH_c and $\ln D_{0c}$ with pressure. The ▲'s are data from Ref. 10.

$$\left(\frac{\partial \ln D_0}{\partial p}\right)_T = \frac{\partial \ln \nu}{\partial p} + \frac{1}{R}\left(\frac{\partial \Delta S}{\partial p}\right)_T = \kappa\gamma + \frac{1}{R}\left(\frac{\partial \Delta S}{\partial p}\right)_T \simeq \frac{1}{R}\left(\frac{\partial \Delta S}{\partial p}\right)_T . \quad (9)$$

Because $\partial \ln D_0/\partial p$ can be determined to an accuracy of only about 10%, the "$\kappa\gamma$" term which is approximately 3% of the second term, is neglected. Thus, by determining $(\partial \ln D_{0c}/\partial p)_T$ and $(\partial \ln D_{0b}/\partial p)_T$, one can obtain values for $(\partial \Delta S_c/\partial p)_T$ and $(\partial \Delta S_b/\partial p)_T$. A linear least-squares analysis of the data of Figs. 6 and 7 gives $(\partial \Delta S_c/\partial p)_T = -(6.0 \pm 0.6)\times 10^{-3}$ cm^3/mole °K and $(\partial \Delta S_b/\partial p)_T = -(6.90 \times 1.0)\times 10^{-3}$ cm^3/mole °K. Therefore, $(\partial \Delta S/\partial p)_T$ appears to be isotropic, to within our experimental uncertainty. An average value for $(\partial \Delta S/\partial p)_T$ is $-(6.5 \pm 0.8)\times 10^{-3}$ cm^3/mole °K and is in good agreement with the value $-(6.4 \pm 0.5)\times 10^{-3}$ cm^3/mole °K obtained for $-(\partial \Delta V/\partial T)_p$ from the data of Fig. 3.

V. DISCUSSION AND INTERPRETATION OF DATA

A. Comparison of Data for α_v with Gilder-Chhabildas Model Calculation

According to the model calculation of Gilder and Chhabildas,[8] well above the Debye temperature, the thermal coefficient of expansion of an activated vacancy, α_v, is given by the following expression:

$$\alpha_v \simeq (R r_0/3\Delta V)(2\kappa_a + \kappa_c)\,\alpha^3 \delta_1^2 \times [545 + (36\sqrt{2}\,\alpha\delta_1)(\delta_2/\delta_1) + 270(\delta_2/\delta_1)^2 - (30/\alpha\delta_1)] , \quad (10)$$

where r_0 is the equilibrium separation of an isolated pair of zinc ions, α^{-1} is a range parameter in a Morse-like potential, and δ_1 and δ_2 are the displacements (assumed to be purely radial) of the first and second nearest neighbors to the vacancy. Using reasonable[8,28] values for α and r_0, the presently measured value of $\Delta V \simeq 4$ cm^3/mole, and a range for δ_2/δ_1 from 0 to 0.5 and δ_1 from $5\times 10^{-2} r_0$ to $10^{-1} r_0$, Eq. (10) places α_v in the range 0.5×10^{-3}–3×10^{-3} °K^{-1}. In the present experiment (see Table IV), α_v varies from 1.7×10^{-3} °K^{-1} at 300.9 °C to 1.5×10^{-2} °K^{-1} at 400.8 °C. In view of the simplifying assumptions made in the calculation, the agreement between the measured values of α_v and those predicted by the theory is indeed satisfactory.

B. Variation of Activation Enthalpy with Pressure

The data of the present experiment indicate that both ΔH_c and ΔH_b are, to within the experimental uncertainty, independent of pressure. The value obtained for $(\partial \Delta H/\partial p)_T$ from the intercept of the ΔV-vs-T plot in Fig. 3 is 0.003 ± 0.3 cm^3/mole. More directly, ΔH_c and ΔH_b obtained from the slopes of the isobars in Figs. 4 and 5, when plotted against pressure, as shown in Figs. 6 and 7, show no variation with pressure to within the experimental uncertainty of about ±0.2 kcal/mole. According to Eq. (8), this result is consistent with $\alpha_v = T^{-1}$, and hence $\Delta V = AT$.

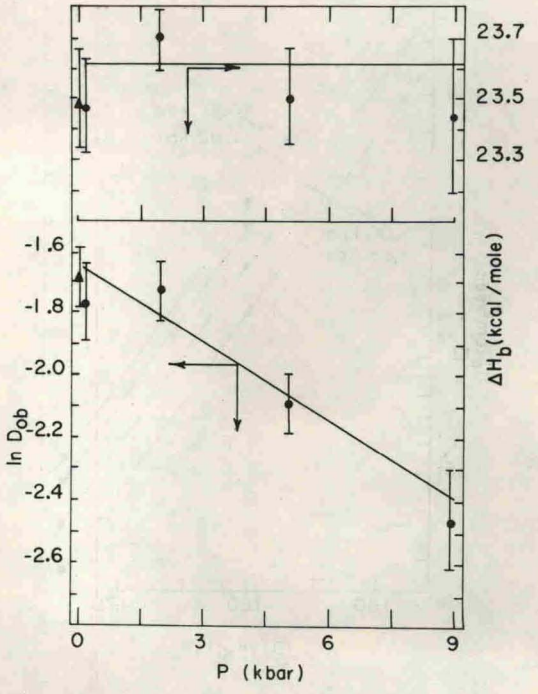

FIG. 7. Variation of ΔH_b and $\ln D_{0b}$ with pressure. The ▲'s are data from Ref. 10.